

Assessment of the ITER baseline operation scenario using CORSICA

S.H. Kim¹, T.A. Casper², J.A. Snipes¹ and A. Loarte¹

¹*ITER Organization, Route de Vinon sur Verdon - CS 90046, 13067 St Paul-Lez-Durance Cedex, France*

²*Woodruff Scientific, Inc. 4000 Aurora Ave N. Ste. 6 Seattle, WA 98103 USA*

Introduction The ITER baseline operation aims at demonstrating controlled burn of deuterium-tritium (D-T) plasmas in the type-I ELM/ H-mode regime and with a high fusion gain ($Q \sim 10$). Improved physics understanding and updated specifications of the ITER components are being continuously integrated to develop more reliable candidate ITER baseline operation scenarios [1-4]. An integrated modelling of the ITER baseline operation including entry to burn, flat-top burning plasma, and exit from burn was previously performed using CORSICA within relatively narrow ranges of plasma parameters and operational conditions [5-6]. In this work, the previously proposed candidate ITER baseline operation scenarios have been further improved with updated modelling features including the confinement mode transitions, peaked density profiles, revised electron cyclotron (EC) heating system configuration, improved edge pedestal modelling and ramp-down shape optimization. Then, the feasibility of these scenarios has been investigated across a range of plasma parameters and operational conditions to take into account the modelling uncertainties.

A baseline operation scenario with a flat density profile shape A 15MA baseline operation scenario, which integrates all the relevant physics, operational constraints, updated modelling features and scenario assumptions, is shown in Figure 1. During the flat-top H-mode phase, the electron density at the pedestal top ($\rho_{\text{tor}} \sim 0.94$) was set to be $9.4 \times 10^{19}/\text{m}^3$ (about 75% of the Greenwald density), in order to allow the core electron density to vary along with the profile peaking factor ($n_0/\langle n_e \rangle = 1.0-1.3$). In the scenario shown in Figure 1, a flat density profile shape ($n_{e0}/\langle n_e \rangle = 1.04$) is assumed and the volume averaged electron density was about $9.4 \times 10^{19}/\text{m}^3$. The fuel isotopes were assumed to be 50:50 DT, and the beryllium (Be) and tungsten (W) impurity concentrations (n_{Be}/n_e and n_{W}/n_e) were assumed to be respectively 0.02 and 1.0×10^{-5} . The effective charge number (Z_{eff}) was about 1.44 during the flat-top phase. The confinement mode transitions were triggered by comparing the power crossing the plasma separatrix (P_{sep}) and the H-mode threshold power estimate ($P_{\text{th,DT}}$) computed using the Martin scaling law [7] and multiplied by 0.8 taking the isotopic mass dependence into account [8-9]. A total of 63MW auxiliary heating power (10MW IC, 33MW NB and 20MW EC) was applied around $t=60$ s to facilitate entry to burn, and then it was reduced to 50MW to optimize the fusion gain (Q) during the burning plasma operation. The fusion power multiplication factor of 10.3 was achieved with the alpha particle self-heating power of about 102MW and plasma confinement enhancement factor (H_{98}) of 1.03. The poloidal flux consumption, CS/PF coil currents and forces were well within their limits.

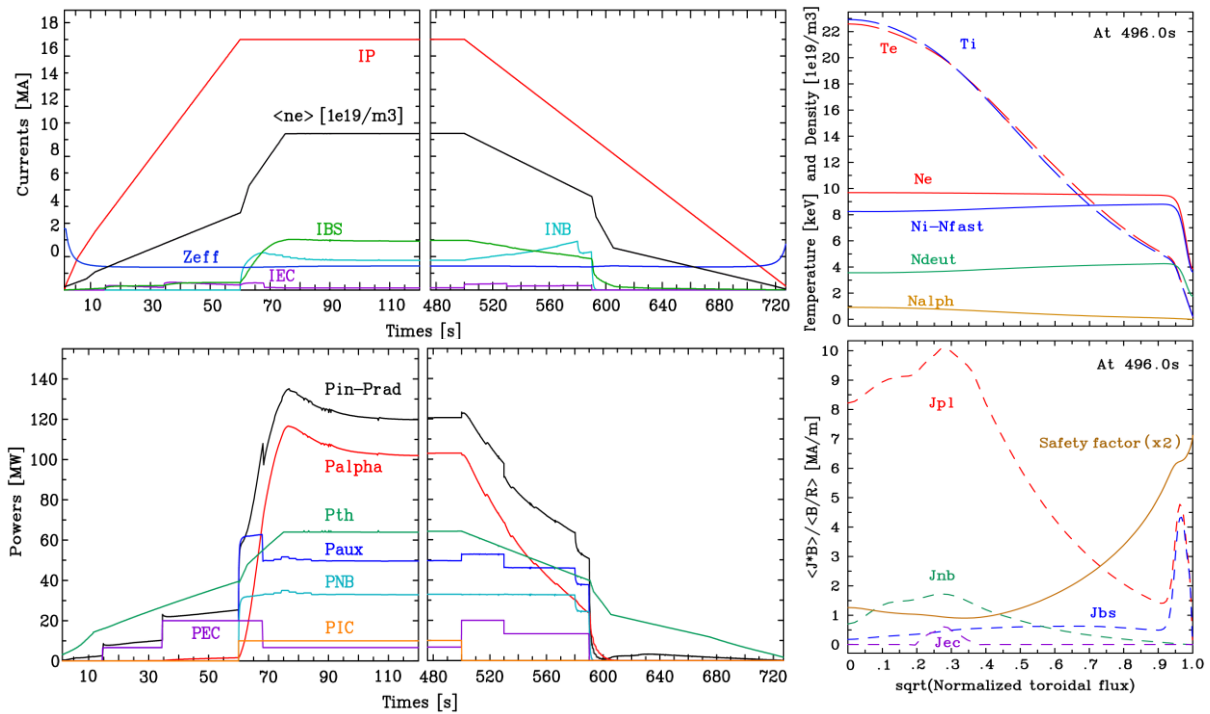


Figure 1. A 15MA baseline operation scenario. Time traces of the plasma current, average electron density, bootstrap and driven currents, and effective charge number (top-left). Time traces of the auxiliary heating power, H-mode threshold power estimate ($P_{th,DT}$) and power crossing the separatrix ($P_{in}-P_{rad}$) (bottom-left). The plasma temperature and density profiles (top-right). The plasma current density and safety factor profiles (bottom-right).

Entry to burn and confinement mode transitions A series of comparative studies performed by varying various scenario modelling assumptions, such as the density evolution time-scale during the confinement mode transitions, H-mode threshold power estimate, confinement mode transition triggering condition and W impurity concentration. Simulations comparing different density evolution time-scales during the confinement mode transitions showed that slower evolution of density is favourable for entry to burn as the increase in the H-mode threshold power becomes slower than the increase in the alpha particle self-heating power [6]. Varying assumptions on the H-mode threshold power estimate showed that a high power margin for reliable H-mode operation could be achieved if the isotopic mass dependence and a potential reduction of the threshold power in a full metal wall environment [8-9] are considered. The uncertainty in projecting the H-mode threshold power scaling to ITER operation needs to be further investigated. A comparison of different confinement mode transition triggering conditions ($P_{sep} \in \{P_{in}, P_{loss}, P_{in}-P_{rad} \text{ and } P_{net}\}$) showed that inclusion of the time derivative of the stored energy (dW/dt) can delay the completion of the confinement mode transitions, if the applied input power waveform (P_{in}) does not vary significantly [10]. Studies on varying the W concentration at different operation conditions (see Table I) showed that the marginal W concentration for H-mode access would be around $2-5 \times 10^{-5}$. These comparative studies collectively indicate that reliable access to the H-mode regime in ITER baseline operation could be achieved across a range of plasma parameters and operational

conditions, if the W concentration is kept below 1.0×10^{-5} and the H-mode threshold power estimate stays in the optimistic range.

Table I. 15MA baseline operation scenarios with various W concentrations. In the first 5 simulations, a constant Be concentration (0.02) is assumed and the isotopic mass dependence is included in the H-mode threshold power estimate. In the next 4 simulations, the effective charge number of 1.7 is assumed while varying W and Be concentrations and the isotopic mass dependence is not included to reflect more challenging baseline operation conditions. Note also that the auxiliary heating power is not optimized for the fusion gain.

$\langle n_W \rangle / \langle n_e \rangle$	$\langle n_{Be} \rangle / \langle n_e \rangle$	Z_{eff}	P_{alpha}	$P_{radiation}$	P_{sep}	P_{aux}	$P_{th,DT} / (P_{th,D})$	$H(L)$	H_{98}	Q
1.0e-7	0.02	1.39	106	23	132	50	65	H	1.00	10.5
1.0e-6	0.02	1.39	106	25	131	50	64	H	1.00	10.6
1.0e-5	0.02	1.44	102	32	119	50	64	H	1.01	10.3
2.0e-5	0.02	1.48	99	40	108	50	64	H	1.03	9.9
5.0e-5	0.02	1.57	8	31	42	50	42	(L)	0.46	0.6
5.3e-7	0.05	1.70	77	32	103	56	(80)	H	1.01	6.8
5.1e-6	0.05	1.70	78	35	100	56	(80)	H	1.01	6.9
2.2e-5	0.04	1.70	79	48	88	56	(80)	H	1.04	6.9
4.0e-5	0.04	1.70	4	21	45	56	(45)	(L)	0.35	0.3

Assessment of the plasma performance Assessment of the flat-top burning plasma performance has been performed by varying the flat-top density and density profile peaking factor, and for two different combinations of main impurity species (Be/Ar and Be/W) to cover a wide range of potential plasma operation conditions. These studies showed that the dependence of the burning plasma performance on the flat-top density and density profile peaking factor can vary depending on the assumed operation conditions. As shown in Figure 2, the alpha particle self-heating power and fusion power multiplication factor were maintained at similar levels when the total radiative power was increased along with the flat-top density (due to a high Ar concentration ($n_{Ar}/n_e \sim 1.35 \times 10^{-3}$) assumed for $Z_{eff} \sim 1.7$), whereas they were linearly increased when a very low W concentration ($n_w/n_e \sim 1.0 \times 10^{-7}$) was assumed for $Z_{eff} \sim 1.4$. Parameter scans on the density profile peaking factor ($n_{e0}/\langle n_e \rangle$) performed without varying the density at the pedestal top showed that operating the plasma with a high density

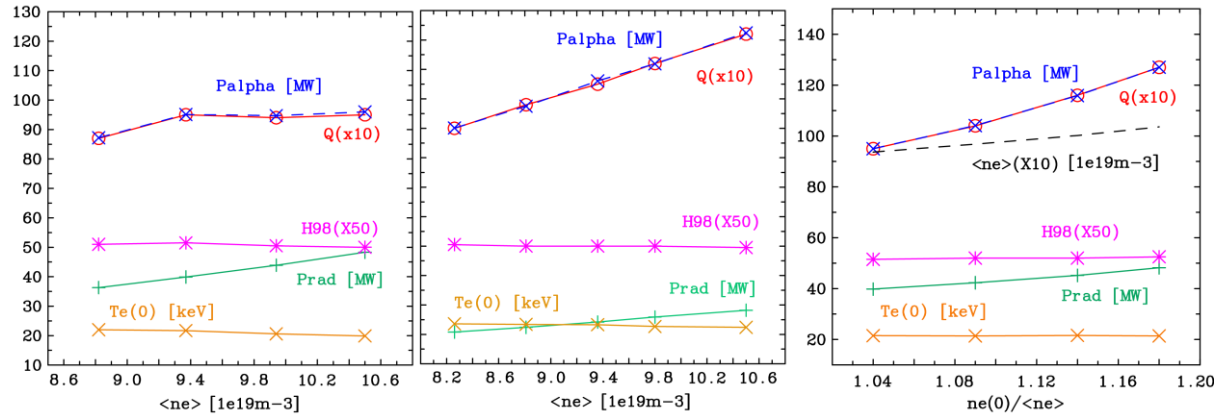


Figure 2. The alpha particle self-heating power, fusion power multiplication factor, confinement enhancement factor, radiative power loss and central electron temperature are compared along the volume averaged electron density. $Z_{eff} \sim 1.7$ is assumed for Be/Ar cases (left), whereas $Z_{eff} \sim 1.4$ is assumed for Be/W cases (right).

Figure 3. Plasma parameters are compared along the electron density profile peaking factor (Be/Ar cases). Similar dependences are also observed in Be/W cases (not shown).

profile peaking factor effectively improves the fusion power multiplication factor (see Figure 3). The core plasma temperatures were not affected by the increase in the core plasma density as the alpha particle self-heating power was also effectively increased at the core region. A comparison of simulations with various combinations of the ITER HCD systems showed that operating 15MA Q=10 ITER baseline operation would be possible if the auxiliary heating power optimized for achieving an H-mode burning plasma operation with $H_{98} \sim 1.0$ can be maintained below 53MW.

Optimization of scenario waveforms Optimization of the current ramp-up and ramp-down has been studied by applying various HCD power waveforms [10]. This study showed that early entry to burn demands the PF6 coil to be operated near its current and field limits whereas late entry reduces the poloidal flux available for the flat-top phase. The shape optimization was important for the ramp-down phase to avoid exceeding the force limits on the coils. Optimization of the current ramp-down phase is continuing to investigate conditions required for a reliable H-L confinement mode transition and plasma termination within the vertical stability margin (see figure 4).

Summary and Conclusions The 15MA ITER baseline operation scenario has been continuously developed by integrating the improved physics modelling features and updated operational constraints, aiming at extending the potential operational window for Q=10 DT burning plasma operation. The improved ITER baseline operation scenarios and analysis results presented in this paper will be a good basis for further investigation and development as the understanding on the burning plasma physics improves.

Acknowledgements The authors wish to thank Drs. R H Bulmer, L L LoDestro, W H Meyer and L D Pearlstein for their support on CORSICA. ITER is the Nuclear Facility INB no. 174. This paper simulates plasma physics processes, neutron production and fusion performance during ITER operation; nevertheless the nuclear operator is not constrained by the results of this paper. The views and opinions expressed herein do not necessarily reflect those of the ITER Organization or its Members.

References

- [1] Parail V *et al* 2013 *Nucl. Fusion* **53** 113002
- [2] Casper T A *et al* 2014 *Nucl. Fusion* **54** 013005
- [3] Kessel C E *et al* 2015 *Nucl. Fusion* **55** 063038
- [4] Koechel F *et al* 2017 *Nucl. Fusion* **57** 086023
- [5] Crotninger J A *et al* 1997 *LLNL Report UCRL-ID-126284*; NTIS #PB2005-102154.
- [6] Kim S H *et al*, 42nd EPS conference on Plasma Phys. Control. Fusion, Lisbon, 2015, ECA Vol.39, P4-170
- [7] Martin Y R *et al* 2008 *Journal of Physics; Conference Series* **123**, 012033
- [8] Righi E *et al* 1999 *Nucl. Fusion* **39** 309
- [9] Ryter F *et al* 2014 *Nucl. Fusion* **54** 083003
- [10] Kim S H *et al*, 2018 *Nucl. Fusion* **58** 056013

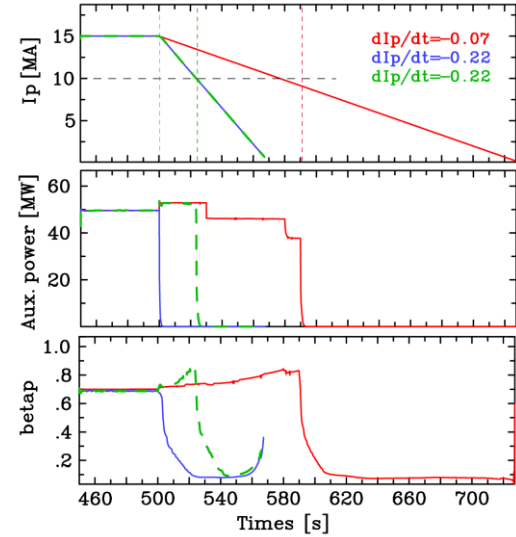


Figure 4. Plasma current ramp-down scenarios with slow or fast current ramp and an H-L transition at 15MA or 10MA. Time traces of the plasma current (top), auxiliary heating power (middle) and poloidal beta (bottom)